Stratosphere-troposphere exchange ozone flux related to deep convection

Q. Tang,[1] M. J. Prather,[1] and J. Hsu[1]

Received 2 November 2010; revised 12 December 2010; accepted 28 December 2010; published 4 February 2011.

[1] We study the mechanisms driving stratosphere-troposphere exchange of ozone fluxes within a chemistry-transport model. For years 2004–2006, year-round, most of the stratosphere-to-troposphere flux of O_3 is associated with shear and folding around the subtropical jet, and this jet-related flux peaks for the northern hemisphere in May. Over the northern mid-latitude continents, however, surface convection penetrates to stratospheric levels of O_3 (250 ppb), enhancing the O_3 flux by 19% of the northern hemisphere total, and shifting the peak flux to June. This convection-related O_3 flux represents 49% of the total over northern mid-latitudes in June. **Citation:** Tang, Q., M. J. Prather, and J. Hsu (2011), Stratosphere-troposphere exchange ozone flux related to deep convection, *Geophys. Res. Lett.*, *38*, L03806, doi:10.1029/2010GL046039.

1. Introduction

[2] Quantifying the exchange of ozone (O_3) and water vapor between the stratosphere and the troposphere is important due to their key roles as greenhouse gases and chemical active species in the upper troposphere and lower stratosphere (UT/LS). Stratosphere-troposphere exchange (STE) is an important term in the budget of tropospheric ozone, determining its interannual variability [*Wild*, 2007; *Voulgarakis et al.*, 2010]. The intensity of stratospheric ozone influx can even affect the ozone abundance at the surface [*Roelofs and Lelieveld*, 1997; *Wild et al.*, 2003; *Wild*, 2007], where exposure to high level ozone has fatal consequence on human health [*Bell et al.*, 2004].

[3] Stratosphere-troposphere exchange is traditionally associated with the jet stream [*Newell*, 1963] and tropopause folds [*Danielsen*, 1968] and is thought to be driven by the large-scale overturning of the stratosphere [*Brewer*, 1949; *Holton et al.*, 1995]. More recently STE has been attributed to mid-latitude deep convection [*Poulida et al.*, 1996; *Fischer et al.*, 2003; *Gray*, 2003; *Hegglin et al.*, 2004]. In these large organized convective systems, the mesoscale ageostrophic movements and tropopause deformation around the convective region result in STE and ozone enhancement in the free troposphere. In addition to these large organized systems, deep convection over summer continents in individual cells is also capable of reaching and/or penetrating the tropopause. In this study, we identify summertime convection over northern hemisphere (NH) continents as crossing the tropopause and producing an enhanced flux of ozone into the troposphere.

[4] Dynamical processes play the dominant role in determining O_3 abundances in the UT/LS region, where transport timescales (days) are shorter than chemical lifetimes (weeks). The mixing of tropospheric and stratospheric air within the extra-tropical tropopause transition layer (ExTL) has been diagnosed by the O_3-CO and O_3-H_2O correlations from various measurements (i.e., the SPURenstofftransport in der Tropopausenregion (SPURT) campaign [*Hoor et al.*, 2004], the Photochemistry of Ozone Loss in the Arctic Region in Summer (POLARIS) campaign [*Pan et al.*, 2007], the Atmospheric Chemistry Experiment Fourier Transform Spectrometer (ACE-FTS) [*Hegglin et al.*, 2009]). The dynamical mechanism of maintaining the sharp gradients in O_3 across the ExTL is still not well understood. Recently, *Miyazaki et al.* [2010] emphasized the importance of small-scale dynamical processes in causing three-dimensional mixing within the ExTL based upon their high-vertical-resolution (~0.3 km) modeling.

[5] In our chemistry-transport modeling (CTM) of ozone [*Tang and Prather*, 2010], we find a small number of convective events reach into the lower stratosphere where O_3 abundances exceed 250 ppb (parts per billion, nanomoles per mole of air), thus eroding the lower stratosphere through direct mixing of tropospheric air and induced subsidence, and driving an STE O_3 flux. The CTM is self-consistent and matches the observed variability in the upper troposphere and lower stratosphere [*Prather et al.*, 2011]. We diagnose the STE flux driven by deep convection and show how it shifts the seasonality of the O_3 flux entering the NH troposphere.

2. Model and Methodology

[6] In this study, the University of California, Irvine (UCI) global off-line CTM is driven by meteorological data from the European Centre for Medium-Range Weather Forecasts (ECMWF) using 3-hour averages of spun-up, pieced-forecasts from the Integrated Forecast System (IFS) as developed by U. Oslo [*Kraabøl et al.*, 2002; *Isaksen et al.*, 2005]. Here, we use meteorological data for years 2004–2006 (IFS cycle 29) at a resolution of T42 (~2.8° × ~2.8° horizontal resolution) L60 (60 layers from surface to 0.02 hPa, about 1 km vertical resolution at the tropopause). The tropospheric chemistry (35 species) uses an updated version of *Carver et al.* [1997] [*Wild et al.*, 2003; *Tang and Prather*, 2010], and the simplified, linearized chemistry for stratospheric ozone is simulated by the linearized ozone scheme (Linoz version 2 [*Hsu and Prather*, 2009]). The tropopause, and hence the switch between the two chemistry modules, is determined naturally by the dynamics and mixing of the meteorological fields using an artificial tracer emitted at the surface [e90, see *Prather et al.*, 2011].

[1]Department of Earth System Science, University of California, Irvine, California, USA.

0094-8276/11/2010GL046039

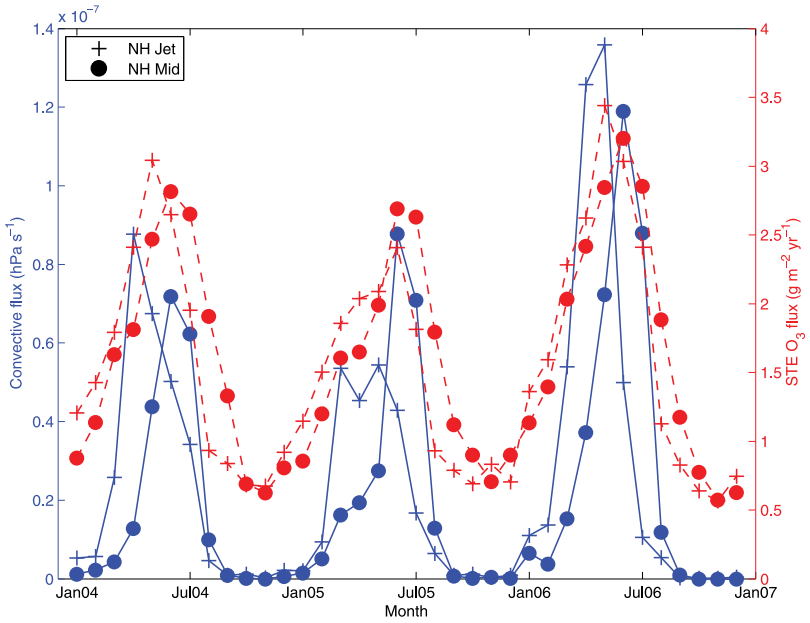

Figure 1. Monthly mean deep convective fluxes (left axis, blue, unit: hPa s^{-1}) and STE O_3 flux (right axis, red, unit: g m^{-2} yr^{-1}) as a function of time (2004–2006) for NH jet (25.1°N–33.5°N, pluses) and mid-latitudes (33.5°N–64.2°N, dots). Convective fluxes are those penetrating the 250-ppb O_3 surface. STE O_3 fluxes are diagnosed across the 120-ppb O_3 surface. 1 g m^{-2} yr^{-1} of global mean flux equals to 510 Tg yr^{-1} globally integrated flux. For convection crossing the 120-ppb O_3 surface, see auxiliary material Figure S1.

[7] The ozone simulations with this CTM at 1° × 1° × L40 resolution have been compared and validated with ozone sondes and satellite observations [*Tang and Prather*, 2010]. The CTM total and tropospheric ozone columns show very good agreement with the Ozone Monitoring Instrument (OMI) data, even on swath-by-swath, pixel-by-pixel basis. The success indicates that the dynamical processes in the UT/LS are well captured by the ECMWF wind fields and the chemical processes are reasonably represented in the CTM. The 1° × 1° met-fields from U. Oslo are only available in a 40-layer version, which has biases in the large-scale stratospheric circulation [*Hsu and Prather*, 2009]. Thus, we opt here for the lower horizontal resolution of T42 but higher vertical resolution of 60 layers, which has better stratospheric circulation and higher vertical resolution in the UT/LS. Both met-fields have similar STE O_3 fluxes (within 10%).

[8] The STE O_3 flux in the UCI CTM is resolved geographically at T42 resolution in this study, and also at the instant the O_3 effectively mixes into the upper troposphere [*Hsu et al.*, 2005; *Hsu and Prather*, 2009]. In this unique diagnostic the tropospheric O_3 mass balance in each grid-square column atmosphere is calculated hourly and includes: net horizontal converge (diagnosed), net photochemical tendency (diagnosed), surface deposition (diagnosed), and net flux from STE (derived). One advantage of this approach over trajectories or related methods is that it is entirely self consistent with respect to ozone chemistry and the meteorology as our transport conserves both total air mass and ozone. With hourly diagnostics, we can accumulate the monthly STE fluxes at the horizontal resolution of the model. There is some unbiased (i.e., zero mean) noise in these calculations because the horizontal flux convergence is not exact, but the integrated global and hemispheric STE are not affected, and the total STE flux diagnosed in this way is confirmed by the total tropospheric O_3 budget.

3. Results

[9] The UCI CTM is spun up by recycling year 2004 wind fields several years to approach a steady state (although with meteorological discontinuity every January 1) and then run continuously from year 2004 through 2006. The results shown here are from the 3-year continuous run. The CTM convective flux uses the 3-hour IFS integration of convective flux updrafts through each layer.

[10] Figure 1 shows the time series of convective updraft mass flux (solid blue) entering grid boxes with $O_3 > 250$ ppb and STE ozone flux (dashed red) across the 120 ppb O_3 isopleth for the northern hemisphere (NH) subtropical jet region (25.1°N–33.5°N, pluses) and middle latitudes (33.5°N–64.2°N, dots). The positive direction of convective flux is from the troposphere to the stratosphere, while the positive direction of STE flux is opposite. All fluxes peak in late spring or early summer, but the jet region (pluses) tends to peak more in the spring while the middle latitudes (dots) more in early summer. STE flux varies interannually with the convective flux, with year 2006 about 25% larger than years 2004 and 2005. From September to December, convection rarely reaches the 250 ppb O_3 surface, but there is still downward STE flux even in mid-latitudes, indicating STE sources other than deep convection, such as tropopause folds [*Danielsen*, 1968; *Sprenger et al.*, 2003], wave breaking [*Scott et al.*, 2001] and cutoff lows [*Ebel et al.*, 1991].

[11] The geographic patterns of convective events and STE flux also show coincidence over summer continents, especially in NH middle latitudes as shown in Figure 2. The summer average for 2005 shows that the region of largest

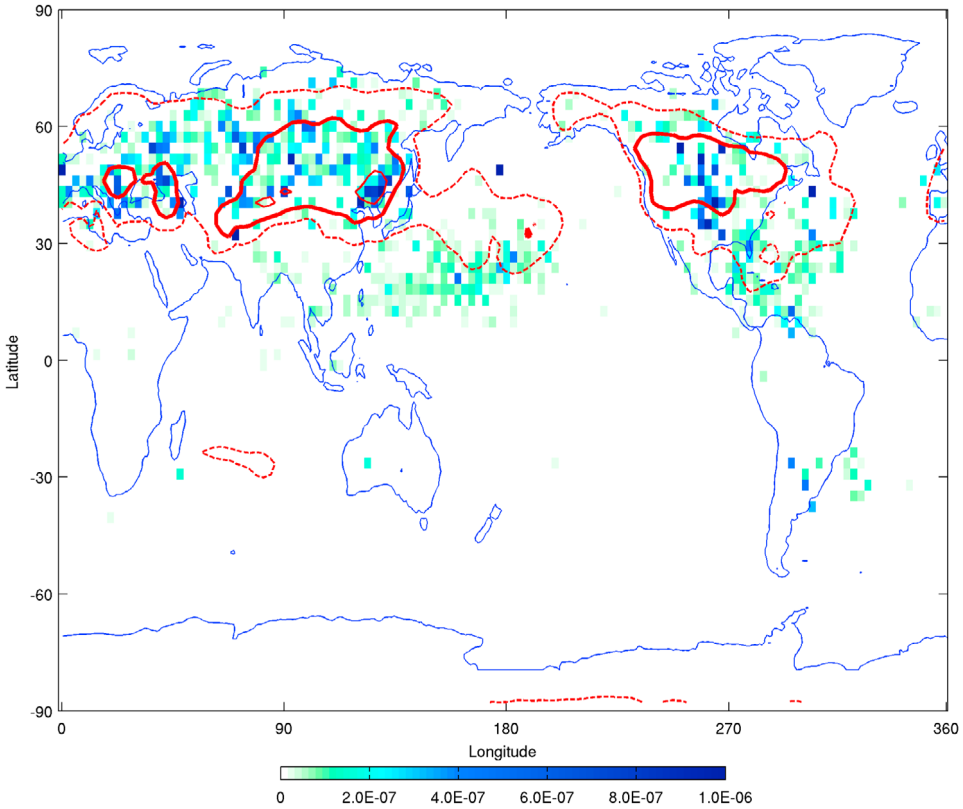

Figure 2. Latitude-longitude plot of mean deep convective fluxes (colored pixels shown at model resolution, unit: hPa s^{-1}) and STE O_3 fluxes (red contour lines, unit: g m^{-2} yr^{-1}) for June, July, and August of 2005. Thick red-solid contour lines represent the STE flux of 3 g m^{-2} yr^{-1}. Red-dashed lines and thin red-solid lines indicate the STE fluxes of 2 and 4 g m^{-2} yr^{-1}, respectively. Deep convective fluxes and STE O_3 fluxes are defined as in Figure 1.

STE O_3 flux (red contour lines) coincides with deep convection (color pixels shown at model resolution). The deep convection diagnosed here clearly crosses the tropopause, whether that boundary is diagnosed from the modeled O_3 or synthetic tracers [*Prather et al.*, 2011]. Convective air masses penetrating into the lower stratosphere will force subsidence, pushing the stratospheric air below it into lower model layers and eventually into the troposphere. We show in Figure 2 that this flux of O_3-rich air enters the troposphere not far from the regions of convection, primarily over the NH continents.

4. Discussion

[12] Many publications have examined the stratosphere-troposphere exchange and the resulting ozone flux, in terms of its magnitude, seasonality and geographic pattern [e.g., *Gettelman et al.*, 1997; *Roelofs and Lelieveld*, 1997; *Olsen et al.*, 2004; *Hsu et al.*, 2005]. Others have examined the meteorological processes that drive STE, such as, tropopause folds near jet streams [*Sprenger et al.*, 2003, Figure 3b], wave breaking [*Scott et al.*, 2001], cutoff lows [*Ebel et al.*, 1991], mid-latitude deep convection [*Poulida et al.*, 1996; *Fischer et al.*, 2003; *Gray*, 2003; *Hegglin et al.*, 2004].

[13] The link between deep convection and the STE O_3 flux has only been found for extreme events on a case-study basis. The results here provide an integrated view and suggest that this relationship between stratosphere-penetrating convection and extra-tropical STE O_3 is pervasive and global. If we re-plot Figure 1 as the monthly fluxes of STE O_3 against those from deep convection (see auxiliary material Figure S2), there are two clear domains for the NH mid-latitudes: a flat line showing monthly variations in STE O_3 when there is little or no deep convection (September to December); and a sloping line showing a near linear relationship between the two when deep convection is present.[1] We posit that the linear regression of the latter data, 490 nanogram O_3 flux across 120-ppb O_3 surface per gram of air convected to O_3 > 250 ppb (r^2 = 0.9), describes a general relationship that applies to all latitudes in this model study and can be used to derive the STE O_3 flux that is attributable to deep convection.

[14] The average of the total and non-convective STE O_3 fluxes (in units of Tg yr^{-1}) are shown as a function of month for each hemisphere in Figure 3. In the NH, the convective STE component peaks in June at 37% of the total and contributes about 19% of the annual total. Deep convection is weaker in the southern hemisphere (SH) and hence the parallel results are 12% for the peak in November and 5% annually. The correlation between convection and STE is more significant over NH middle latitudes than NH subtropical jet regions, and in spring and summer than in fall

[1] Auxiliary materials are available in the HTML. doi:10.1029/2010GL046039.

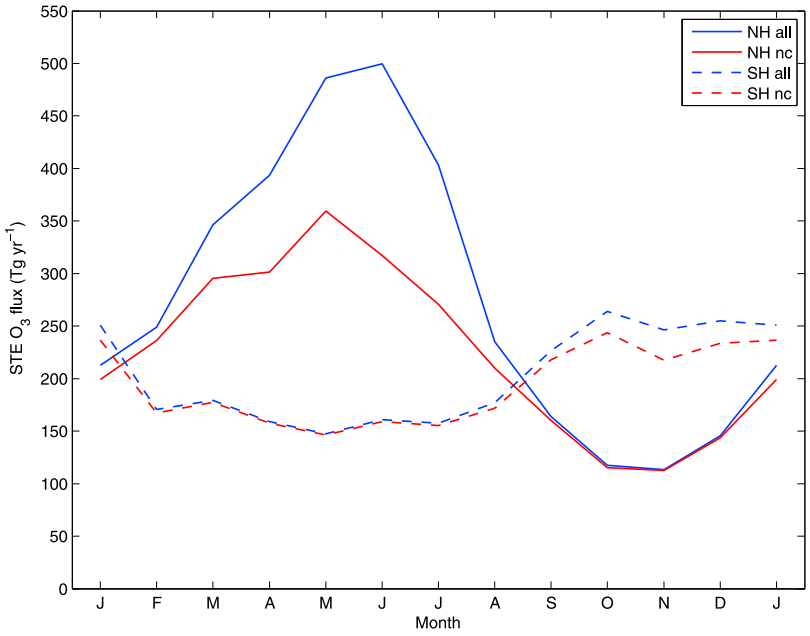

Figure 3. Monthly mean STE O_3 fluxes (unit: Tg yr^{-1}) for years 2004–2006 as a function of month. For the NH, the total STE (solid-blue line) is compared with the STE without convective component (solid-red line). Parallel results are shown for the SH (dashed lines). In the NH, the STE O_3 fluxes are 281 and 54 Tg yr^{-1} for the total and convective component, respectively. The fluxes are 200 and 9 Tg yr^{-1} in the SH. Deep convective fluxes and STE O_3 fluxes are defined as in Figure 1.

and winter. In the NH the convectively driven flux shifts the phase of the maximum STE O_3 flux from May to June. Over the mid-latitude continents, the non-convective STE O_3 flux is flat for six months (March–August), but convection enhances the peak of total flux in June–July (see auxiliary material Figure S3).

5. Conclusions

[15] Deep convection in the model is shown here to be extensive and ubiquitous over the northern continents in summer. Our ability to diagnose the geographical locations of STE O_3 flux clearly identifies stratosphere-penetrating convection as an important factor of summertime tropospheric O_3 in the northern mid-latitudes. Indeed, the O_3 maximum in the upper troposphere identified by Logan [see *Logan*, 1999, Figure 8] that is found over continents in the NH mid-latitudes (i.e., the sonde sites) occurs in June, and is consistent with the deep convective STE flux.

[16] An upward shift of the extra-tropical tropopause height and a poleward migration of jet streams have been associated with increased abundance of greenhouse gases and stratospheric ozone depletion and global warming [*Kushner et al.*, 2001; *Santer et al.*, 2003; *Lorenz and DeWeaver*, 2007]. The anticipated climate change over the 21st century is projected to enhance the STE O_3 flux based primarily on a changing stratospheric circulation [e.g., *Sudo et al.*, 2003; *Eyring et al.*, 2007; *Oman et al.*, 2010]. It is unclear how all these changes will alter the STE flux over continents that contributes to surface ozone levels during peak pollution periods in summer. Assessment of the importance of changing STE O_3 flux should comprise all mechanisms, including tropospheric convection, and evaluate the importance of location and timing in terms of air quality and greenhouse gas forcing by tropospheric ozone.

[17] **Acknowledgments.** This research was supported by NSF Atmospheric Chemistry (ATM-0550234) and NASA MAP/GMI (NNG06GB84G and NNX09AJ47G).

References

Bell, M. L., A. McDermott, S. L. Zeger, J. M. Samet, and F. Dominici (2004), Ozone and short-term mortality in 95 US urban communities, 1987–2000, *JAMA, J. Am. Med. Assoc.*, *292*(19), 2372–2378.

Brewer, A. W. (1949), Evidence for a world circulation provided by the measurements of helium and water vapour distribution in the stratosphere, *Q. J. R. Meteorol. Soc.*, *75*(326), 351–363.

Carver, G., P. Brown, and O. Wild (1997), The ASAD atmospheric chemistry integration package and chemical reaction database, *Comput. Phys. Commun.*, *105*, 197–215.

Danielsen, E. F. (1968), Stratospheric-tropospheric exchange based on radioactivity, ozone and potential vorticity, *J. Atmos. Sci.*, *25*, 502–518.

Ebel, A., H. Hass, H. Jakobs, M. Laube, M. Memmesheimer, A. Oberreuter, H. Geiss, and Y.-H. Kuo (1991), Simulation of ozone intrusion caused by a tropopause fold and cut-off low, *Atmos. Environ., Part A*, *25*(10), 2131–2144, doi:10.1016/0960-1686(91)90089-P.

Eyring, V., et al. (2007), Multimodel projections of stratospheric ozone in the 21st century, *J. Geophys. Res.*, *112*, D16303, doi:10.1029/2006JD008332.

Fischer, H., et al. (2003), Deep convective injection of boundary layer air into the lowermost stratosphere at midlatitudes, *Atmos. Chem. Phys.*, *3*(3), 739–745, doi:10.5194/acp-3-739-2003.

Gettelman, A., J. R. Holton, and K. H. Rosenlof (1997), Mass fluxes of O_3, CH_4, N_2O and CF_2Cl_2 in the lower stratosphere calculated from observational data, *J. Geophys. Res.*, *102*(D15), 19,149–19,159, doi:10.1029/97JD01014.

Gray, S. L. (2003), A case study of stratosphere to troposphere transport: The role of convective transport and the sensitivity to model resolution, *J. Geophys. Res.*, *108*(D18), 4590, doi:10.1029/2002JD003317.

Hegglin, M. I., et al. (2004), Tracing troposphere-to-stratosphere transport above a mid-latitude deep convective system, *Atmos. Chem. Phys.*, *4*(3), 741–756, doi:10.5194/acp-4-741-2004.

Hegglin, M. I., C. D. Boone, G. L. Manney, and K. A. Walker (2009), A global view of the extratropical tropopause transition layer from Atmospheric Chemistry Experiment Fourier Transform Spectrometer O_3, H_2O, and CO, *J. Geophys. Res.*, *114*, D00B11, doi:10.1029/2008JD009984.

Holton, J. R., P. H. Haynes, M. E. McIntyre, A. R. Douglass, R. B. Rood, and L. Pfister (1995), Stratosphere-troposphere exchange, *Rev. Geophys.*, *33*(4), 403–439.

Hoor, P., C. Gurk, D. Brunner, M. I. Hegglin, H. Wernli, and H. Fischer (2004), Seasonality and extent of extratropical TST derived from in-situ CO measurements during SPURT, *Atmos. Chem. Phys.*, *4*(5), 1427–1442, doi:10.5194/acp-4-1427-2004.

Hsu, J., and M. J. Prather (2009), Stratospheric variability and tropospheric ozone, *J. Geophys. Res.*, *114*, D06102, doi:10.1029/2008JD010942.

Hsu, J., M. J. Prather, and O. Wild (2005), Diagnosing the stratosphere-to-troposphere flux of ozone in a chemistry transport model, *J. Geophys. Res.*, *110*, D19305, doi:10.1029/2005JD006045.

Isaksen, I. S. A., C. Zerefos, K. Kourtidis, C. Meleti, S. B. Dalsoren, J. K. Sundet, A. Grini, P. Zanis, and D. Balis (2005), Tropospheric ozone changes at unpolluted and semipolluted regions induced by stratospheric ozone changes, *J. Geophys. Res.*, *110*, D02302, doi:10.1029/2004JD004618.

Kraabøl, A. G., T. K. Berntsen, J. K. Sundet, and F. Stordal (2002), Impacts of NO_x emissions from subsonic aircraft in a global three-dimensional chemistry transport model including plume processes, *J. Geophys. Res.*, *107*(D22), 4655, doi:10.1029/2001JD001019.

Kushner, P. J., I. M. Held, and T. L. Delworth (2001), Southern hemisphere atmospheric circulation response to global warming, *J. Clim.*, *14*(10), 2238–2249.

Logan, J. A. (1999), An analysis of ozonesonde data for the troposphere: Recommendations for testing 3-D models and development of a gridded climatology for tropospheric ozone, *J. Geophys. Res.*, *104*(D13), 16,115–16,149.

Lorenz, D. J., and E. T. DeWeaver (2007), Tropopause height and zonal wind response to global warming in the IPCC scenario integrations, *J. Geophys. Res.*, *112*, D10119, doi:10.1029/2006JD008087.

Miyazaki, K., S. Watanabe, Y. Kawatani, K. Sato, Y. Tomikawa, and M. Takahashi (2010), Transport and mixing in the extratropical tropopause region in a high-vertical-resolution GCM. Part II: Relative importance of large-scale and small-scale dynamics, *J. Atmos. Sci.*, *67*(5), 1315–1336, doi:10.1175/2009JAS3334.1.

Newell, R. E. (1963), Transfer through the tropopause and within the stratosphere, *Q. J. R. Meteorol. Soc.*, *89*(380), 167–204.

Olsen, M. A., M. R. Schoeberl, and A. R. Douglass (2004), Stratosphere-troposphere exchange of mass and ozone, *J. Geophys. Res.*, *109*, D24114, doi:10.1029/2004JD005186.

Oman, L. D., et al. (2010), Multi-model assessment of the factors driving stratospheric ozone evolution over the 21st century, *J. Geophys. Res.*, *115*, D24306, doi:10.1029/2010JD014362.

Pan, L. L., J. C. Wei, D. E. Kinnison, R. R. Garcia, D. J. Wuebbles, and G. P. Brasseur (2007), A set of diagnostics for evaluating chemistry-climate models in the extratropical tropopause region, *J. Geophys. Res.*, *112*, D09316, doi:10.1029/2006JD007792.

Poulida, O., R. R. Dickerson, and A. Heymsfield (1996), Stratosphere-troposphere exchange in a midlatitude mesoscale convective complex, *J. Geophys. Res.*, *101*(D3), 6823–6836.

Prather, M. J., X. Zhu, Q. Tang, J. Hsu, and J. L. Neu (2011), An atmospheric chemist in search of the tropopause, *J. Geophys. Res.*, doi:10.1029/2010JD014939, in press.

Roelofs, G. J., and J. Lelieveld (1997), Model study of the influence of cross-tropopause O_3 transports on tropospheric O_3 levels, *Tellus B*, *49*(1), 38–55.

Santer, B. D., et al. (2003), Contributions of anthropogenic and natural forcing to recent tropopause height changes, *Science*, *301*(5632), 479–483.

Scott, R. K., J. P. Cammas, P. Mascart, and C. Stolle (2001), Stratospheric filamentation into the upper tropical troposphere, *J. Geophys. Res.*, *106*(D11), 11,835–11,848.

Sprenger, M., M. C. Maspoli, and H. Wernli (2003), Tropopause folds and cross-tropopause exchange: A global investigation based upon ECMWF analyses for the time period March 2000 to February 2001, *J. Geophys. Res.*, *108*(D12), 8518, doi:10.1029/2002JD002587.

Sudo, K., M. Takahashi, and H. Akimoto (2003), Future changes in stratosphere-troposphere exchange and their impacts on future tropospheric ozone simulations, *Geophys. Res. Lett.*, *30*(24), 2256, doi:10.1029/2003GL018526.

Tang, Q., and M. J. Prather (2010), Correlating tropospheric column ozone with tropopause folds: the Aura-OMI satellite data, *Atmos. Chem. Phys.*, *10*(19), 9681–9688, doi:10.5194/acp-10-9681-2010.

Voulgarakis, A., N. H. Savage, O. Wild, P. Braesicke, P. J. Young, G. D. Carver, and J. A. Pyle (2010), Interannual variability of tropospheric composition: the influence of changes in emissions, meteorology and clouds, *Atmos. Chem. Phys.*, *10*(5), 2491–2506, doi:10.5194/acp-10-2491-2010.

Wild, O. (2007), Modelling the global tropospheric ozone budget: Exploring the variability in current models, *Atmos. Chem. Phys.*, *7*(10), 2643–2660, doi:10.5194/acp-7-2643-2007.

Wild, O., J. Sundet, M. Prather, I. Isaksen, H. Akimoto, E. Browell, and S. Oltmans (2003), Chemical transport model ozone simulations for spring 2001 over the western Pacific: Comparisons with TRACE-P lidar, ozonesondes, and total ozone mapping spectrometer columns, *J. Geophys. Res.*, *108*(D21), 8826, doi:10.1029/2002JD003283.

J. Hsu, M. J. Prather, and Q. Tang, Department of Earth System Science, University of California, Irvine, CA 92697, USA. (tangq@uci.edu)